OPEN ACCESS

Acoustic metamaterials for new two-dimensional sonic devices

New Journal of Physics
The open-access journal for physics

Acoustic metamaterials for new two-dimensional sonic devices

Daniel Torrent and José Sánchez-Dehesa[1]
Wave Phenomena Group, Department of Electronic Engineering,
Polytechnic University of Valencia, C/Camino de Vera sn,
E-46022 Valencia, Spain
E-mail: jsdehesa@upvnet.upv.es

New Journal of Physics **9** (2007) 323
Received 18 July 2007
Published 11 September 2007
Online at http://www.njp.org/
doi:10.1088/1367-2630/9/9/323

Abstract. It has been shown that two-dimensional arrays of rigid or fluidlike cylinders in a fluid or a gas define, in the limit of large wavelengths, a class of acoustic metamaterials whose effective parameters (sound velocity and density) can be tailored up to a certain limit. This work goes a step further by considering arrays of solid cylinders in which the elastic properties of cylinders are taken into account. We have also treated mixtures of two different elastic cylinders. It is shown that both effects broaden the range of acoustic parameters available for designing metamaterials. For example, it is predicted that metamaterials with perfect matching of impedance with air are now possible by using aerogel and rigid cylinders equally distributed in a square lattice. As a potential application of the proposed metamaterial, we present a gradient index lens for airborne sound (i.e. a sonic Wood lens) whose functionality is demonstrated by multiple scattering simulations.

[1] Author to whom any correspondence should be addressed.

PII: S1367-2630(07)55377-2

Contents

1. Introduction 2
2. Asymptotic expression for the T matrix of an elastic cylinder embedded in a fluid 3
3. Homogenization of 2D arrays of elastic cylinders in a fluid or gas 5
4. *Zc* phase diagrams for metamaterials based on 2D mixtures of two different solid cylinders embedded in a fluid 8
5. Application: a gradient-index sonic lens 11
6. Summary 12
Acknowledgments 13
References 13

1. Introduction

Periodic distributions of sound scatterers in air or a fluid, also called sonic crystals (SC), have been employed to demonstrate novel physical phenomena like, for example, focusing by two-dimensional (2D) arrays of rigid cylinders in air [1], negative refraction by 3D distributions of solid spheres in water [2] or negative dynamic bulk modulus achieved by 1D array of Helmholtz resonators in water [3]. Moreover, the behavior of SC in the regime of large wavelengths (large in comparison with the separation between the scatterers) is a topic of increasing interest. In this regime, the SC behave as effective homogeneous acoustic metamaterials whose parameters (sound velocity, c^* and dynamical mass density ρ^*) are mainly determined by the fraction of volume occupied by the scatterers and their refractive properties have been studied by several groups [1], [4]–[11]. Therefore, metamaterials with a prefixed dynamical mass density and sound velocity can be tailored within certain limitations. For example, the cluster of rigid cylinders in air employed in the construction of the sonic lens reported in [1] effectively behaves as an acoustic metamaterial with refractive index $n^* \approx 1.3$. More recently, acoustic metamaterials with very small acoustic impedance Z^* $(= \rho^* c^*)$ mismatch with air have been proposed [7] to enhance the performance of the sonic lenses based on them. However, its practical realization is still lacking.

This work introduces an analytical theory allowing the design of acoustic metamaterials whose parameters, c^* and ρ^*, both being positive can be tailored with practically no limitation by properly choosing the materials employed in the construction and their spatial distribution. An important characteristic of the metamaterials here proposed is the feasibility for a practical realization and their potential for device applications. Thus, an acoustic metamaterial will be introduced consisting of a mixing of aerogel (Gel) and aluminium (Al) cylinders distributed in a square array such that its acoustic impedance perfectly matches that of air and its refractive index is adjustable with the cylinders' radii. Among the possible interesting devices in which this property can be used, here we will report the design of a broadband gradient index 2D sonic lens producing sound focusing with intensity much larger than those previously reported, which were based either on curved-shaped SC clusters [1] or on a cluster with flat surfaces optimized by a genetic algorithm [12]. This work represents a first attempt to get acoustic metamaterials needed to achieve cloaking for acoustic waves [13] as has been previously proposed for electromagnetic waves [14, 15].

This paper is organized as follows. First, in section 2, we present the expansion of the T matrix elements in the low frequency limit. These results are employed in section 3, which studies the homogenization properties of elastic cylinders embedded in a fluid or a gas. Here, different behaviors of physical interest will be analyzed with the help of $c\rho$ phase diagrams. Afterward, section 4 demonstrates that the possibilities of metamaterial design broadens by mixing two different elastic materials in the lattice; Zc phase diagrams will be introduced to help in the selection of metamaterial properties and it will be shown that the possibility of designing novel acoustic devices increases by a large amount. As a possible application of the selected metamaterial, section 5 presents the simulation of a gradient index sonic lens for airborne sound based on an acoustic metamaterial with perfect matching of impedance with air. The paper ends with a summary in section 6.

2. Asymptotic expression for the T matrix of an elastic cylinder embedded in a fluid

In the low frequency limit ($\omega \to 0$), the expansion of the T matrix (in powers of the wavenumber k) for a fluidlike cylinder embedded in a fluid or a gas background was recently reported by us [10]. This section is devoted to the analogous problem but for the case of a solid cylinder (which will support shear waves in addition to compressional waves). The scattering of sound by solid cylinders and spheres embedded in a fluid was studied in the fifties by Faran [16], however, the expressions for the lower order elements of the k-expansion of the corresponding T matrix have not been reported yet.

Let us consider an infinitely long elastic cylinder of radius R_0, Lamé coefficients λ_a and μ_a and density ρ_a immersed in a nonviscous fluid or gas with density ρ_b and speed of sound c_b. Also, let us assume that the cylinder is located at the origin of coordinates with the axis of the cylinder being oriented along the z-axis. If some external harmonic acoustic field of frequency, ω, and wavenumber $k = \omega/c_b$ impinges the cylinder, the total pressure at any arbitrary point (r, θ) of the 2D space in polar coordinates, will be the addition of external (P^{ext}) and scattered (P^{scat}) pressures:

$$P(r,\theta;k) = P^{\text{ext}}(r,\theta;k) + P^{\text{scat}}(r,\theta;k) = \sum_q A_q^0 J_q(kr)\mathrm{e}^{\mathrm{i}q\theta} + \sum_q A_q H_q(kr)\mathrm{e}^{\mathrm{i}q\theta}, \tag{1}$$

where A_q^0 and A_q are the external and scattered coefficients, respectively. $J_q(\cdot)$ and $H_q(\cdot)$ are the qth order Bessel function and Hankel function of first kind, respectively. The relationship between the coefficients of the incident wave A_q^0 and the scattered wave A_q, defines the T matrix of the problem [17]; i.e. $\mathcal{A} = \mathcal{T}\mathcal{A}^0$.

The boundary conditions at the interface between an elastic cylinder and the fluid/gas background are described in textbooks and also can be found, for example, in [16]. After a few manipulations, the relationship between coefficients for the case of circular shaped cylinders is:

$$A_q = -\frac{\rho_q J_q'(kR_0) - J_q(kR_0)}{\rho_q H_q'(kR_0) - H_q(kR_0)} A_q^0 \equiv T_{qq} A_q^0. \tag{2}$$

This T matrix is diagonal and has the same functional form as that obtained for circular shaped fluidlike cylinder (see equations (A.1) and (A.2) in [10]); the important difference being the factor ρ_q, which has now a more complex form:

$$\rho_q \equiv \frac{\rho_a}{\rho_b} k c_b^2 \frac{I_q}{G_q}, \tag{3}$$

where

$$I_q \equiv \frac{\mathrm{i}q}{R_0} F_q J_q(k_t R_0) - k_l J_q'(k_l R_0), \tag{4}$$

$$G_q \equiv \frac{2\mathrm{i}q\mu_a}{R_0^2} F_q \left[J_q(k_t R_0) - k_t R_0 J_q'(k_t R_0) \right] - k_l^2 \left[\lambda_a J_q(k_l R_0) - 2\mu_a J_q''(k_l R_0) \right], \tag{5}$$

$$F_q \equiv \frac{2\mathrm{i}q}{k_t^2 R_0^2} \left[\frac{J_q(k_l R_0) - k_l R_0 J_q'(k_l R_0)}{J_q(k_t R_0) + 2 J_q''(k_t R_0)} \right]. \tag{6}$$

At long wavelengths, the asymptotic expressions of the Bessel and Hankel functions for $k \to 0$ allow to obtain the lower order elements, $\hat{T}_{qq}$, of the series expansion for the T matrix elements above. The derivation is straightforward and details are not given. The reader should consult [10] to follow the rigorous derivation reported for the case of a fluidlike cylinder.

Thus, for the matrix element $q = 0$, the following result is obtained

$$\hat{T}_{00} \equiv \lim_{k\to 0} \frac{T_{00}}{k^2} = \frac{\mathrm{i}\pi R_0^2}{4} \left[\frac{\rho_\mathrm{b} c_\mathrm{b}^2}{\rho_\mathrm{a}(c_\ell^2 - c_\mathrm{t}^2)} - 1 \right]. \tag{7}$$

Note that this element is similar to that of a fluidlike cylinder [10] in which the sound speed is replaced by

$$c_\mathrm{a} \equiv \sqrt{c_\ell^2 - c_\mathrm{t}^2} = \sqrt{\frac{\lambda_\mathrm{a} + \mu_\mathrm{a}}{\rho_\mathrm{a}}}, \tag{8}$$

where the quantity $\lambda_\mathrm{a} + \mu_\mathrm{a}$ is also called the area bulk modulus B_a, which is obtained from the 2D version of the elasticity equations [18]. It is interesting to remember that the bulk modulus in a 3D system is $B_\mathrm{a}^{3\mathrm{D}} = \lambda_\mathrm{a} + 2/3\mu_\mathrm{a}$. Also, let us remark that the theory developed in [10], based in the multiple scattering of sound, leads to a 2D version of Wood's law [19]

$$\frac{1}{B^*} = \frac{f}{B_\mathrm{a}} + \frac{1-f}{B_\mathrm{b}}. \tag{9}$$

The asymptotic form for the element $q = 1$ is

$$\hat{T}_{11} \equiv \lim_{k\to 0} \frac{T_{11}}{k^2} = \frac{i\pi R_0^2}{4} \frac{\rho_\mathrm{a} - 1}{\rho_\mathrm{a} + 1}, \tag{10}$$

which is the same as a fluid cylinder with density ρ_a (see equation (28) in [10]).

Finally, for the elements with $q > 1$

$$\hat{T}_{qq} \equiv \lim_{k\to 0} \frac{T_{qq}}{k^{2|q|}} = \frac{\mathrm{i}\pi R_0^{2q}}{4^q} \frac{1}{q!(q-1)!}. \tag{11}$$

In comparison with those corresponding to a fluidlike cylinder, the factor $(\rho_\mathrm{a} - 1)/(\rho_\mathrm{a} + 1)$ is lacking (see equation (A.3*b*) in [10]).

It is important to point out that for $\rho_\mathrm{a} \to \infty$, the elements above converge to those obtained by solving the case of a rigid cylinder (where no waves are allowed inside the cylinder).

To summarize this section, it can be concluded that an elastic cylinder can be approximately considered (in the long wavelength limit) as a fluidlike cylinder of density equal to that of the elastic material but with an effective speed of sound given by (8). Once the low frequency expansion for the T matrix of a single solid cylinder is known, the homogenization of clusters based on them can be treated as explained below.

3. Homogenization of 2D arrays of elastic cylinders in a fluid or gas

The homogenization method previously developed to obtain the effective acoustic parameters of clusters made of 2D distributions of fluidlike cylinders embedded in a nonviscous fluid or gas [9]–[11] is here extended to clusters made of solid cylinders and, therefore, the full elastic properties of cylinders are taken into account. It is shown that these clusters lead to effective isotropic media (metamaterials) in which sound travels with a speed that can be larger or smaller than that of the surrounding medium depending on the elastic parameters and the volume fraction occupied by the cylinders in the lattice (i.e. its filling fraction, f). Moreover, phase diagrams are introduced to establish (in the ρc-plane) the metamaterial properties as a function of the elastic parameters of cylinders and its filling fraction in the corresponding SC.

It has been proved [10] that the elements $\hat{T}_{00}$ and $\hat{T}_{11}$ are enough to characterize the homogenization of SC based on fluidlike cylinders. Also, the previous section has demonstrated that there is a close analogy between the T matrix elements of solid and fluidlike cylinders. Thus, the $\hat{T}_{00}$ and $\hat{T}_{11}$ elements of a solid cylinder are equal to those of a fluidlike cylinder that has a sound speed given by $c_a \equiv \sqrt{c_\ell^2 - c_t^2}$, where c_ℓ and c_t are, respectively the longitudinal and transversal velocities of the actual elastic cylinder. Therefore, the effective parameters of SC made of 2D binary solid(cylinders)–fluid(background) composites can be obtained from the general expressions already reported for 2D fluid–fluid composites.

In what follows, we will discuss the behavior (in the homogenization limit) of c^*, the effective velocity of sound propagating in a SC consisting of a square distribution of solid cylinders in water as a function of f. In regards to the effective mass density, ρ^*, its behavior is monotonic between that of the background ρ_b at $f = 0$ and a final ρ_{CP} (that approaches that of the solid, ρ_a) at the condition of close-packing, $f = f_{CP}$. This behavior is of little interest and will not be discussed here.

Hereafter, an overlined variable denotes the corresponding quantity normalized to that of the background; for example, $\overline{\rho} \equiv \rho/\rho_b$ and $\overline{c} \equiv c/c_b$.

In brief, at long wavelengths, a 2D array of elastic cylinders embedded in a fluid or a gas defines an acoustic metamaterial in which sound travels with a speed $\overline{c}^*$ determined by (see section 2 and equation (33) in [10]):

$$\frac{1}{\overline{c}^{*2}} = \left[\frac{f}{\overline{\rho}_a \overline{c}_a^2} + (1-f)\right] \cdot \frac{\overline{\rho}_a(\Delta + f) + (\Delta - f)}{\overline{\rho}_a(\Delta - f) + (\Delta + f)}, \tag{12}$$

where c_a is given by equation (8) and the Δ factor contains information about the material parameters of cylinders, their positions in the 2D space and their mutual interaction (see equation (31) in [10]). As in the case of 2D fluid–fluid composites, the value of Δ is different from 1 only for large f.

Figure 1 plots the three possible behaviors expected for $\overline{c}^*$ as a function of f. When the cylinders are made of lead (Pb), $\overline{c}^*$ is always lower than one; a behavior similar to that found for rigid cylinders [1, 4, 9], and it is due to the huge acoustic impedance of Pb relative to that of water. However, for the Al case, $\overline{c}^*$ is always higher than one due to the low ratio of acoustic impedances Z_a/Z_b. Finally, the case of iron (Fe) cylinders is an intermediate case; $\overline{c}^*$ is lower than one for low f and higher than 1 for f large enough. The elastic parameters of the materials employed in the calculations here are listed in table 1.

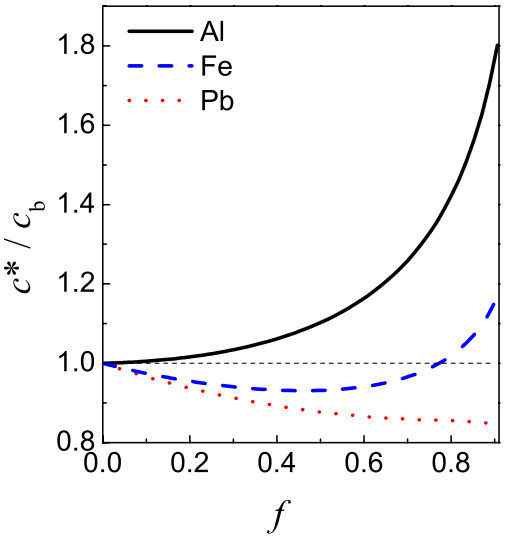

Figure 1. Speed of sound in a 2D acoustic metamaterial consisting of a square configuration of solid cylinders in water. The calculated effective sound speed, c^*, relative to that of water, c_b is plotted as a function of the filling fraction, f. Three different behaviors are possible when f increases: (i) a continuous decreasing of velocity as in the case of Pb, (ii) a continuous increasing of velocity as in the case of Al and (iii) an initial decreasing that with increasing f becomes a velocity larger than the background as for Fe cylinders. The horizontal dashed line is a guide for the eye that defines the condition, $c^* = c_b$.

As explained above, a variety of behaviors is expected for c^* depending on the material composition of cylinders and their filling fraction in the SC. This phenomenon motivates the introduction of some kind of phase diagrams for 2D elastic–fluid composites. It turns out that the condition $\overline{c}^* > 1$ leads to the following relation (assuming $\Delta = 1$) between the cylinder's fluidlike speed of sound, $\overline{c}_a$, its density $\overline{\rho}_a$ and f

$$\overline{c}_a^2 > \frac{1}{\overline{\rho}_a} \cdot \frac{(1-f)+(1+f)\overline{\rho}_a}{(3-f)-(1-f)\overline{\rho}_a}. \tag{13}$$

The color lines in figure 2 represent the separation between the two possible 'phases' of the metamaterial according to the value of $\overline{c}^*$ (higher or lower than 1). They are plotted for four different f in the $\overline{\rho}_a\overline{c}_a$-plane. It is shown that these lines are always above the region $\overline{c}_a = 1$, which means that $\overline{c}^*$ cannot obtain a value higher than one if c_a is lower than that of the surrounding medium.

Note that all the lines become vertical in the limit

$$\overline{\rho}_a \to \frac{3-f}{1-f}. \tag{14}$$

Thus, $\overline{c}^* < 1$ when $\overline{c}_a \geqslant 3$ and $\overline{\rho}_a \geqslant (3-f)/(1-f)$. In more general terms, it can be said that lines associated to a given f separate the region in which the metamaterial behaves with $\overline{c}^* > 1$ (upper-left region) from the one in which $\overline{c}^* < 1$ (lower-right region).

The black dots in figure 2, represent the elastic properties of several materials commonly used in building SC. According to their positions in the $\overline{\rho}_a\overline{c}_a$-plane, it is concluded that: (i) SC

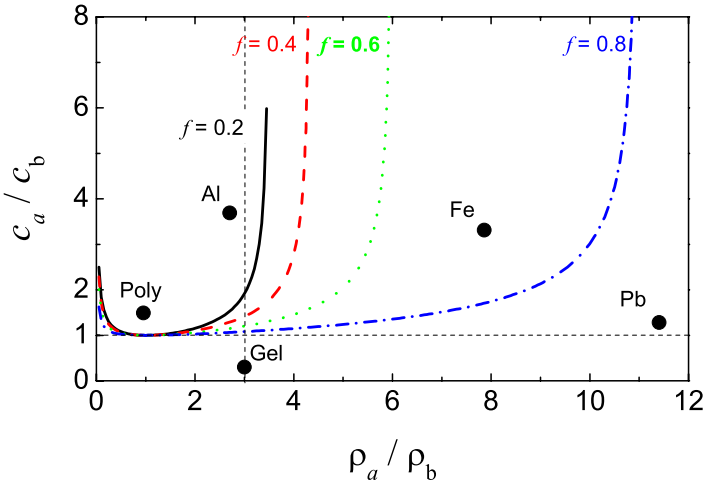

Figure 2. $c\rho$ phase diagram of acoustic metamaterials based on SC made of a square configuration of one single component full of elastic cylinders. For the given fraction of volume occupied by the cylinders in the lattice (f), the corresponding color line separates the region where the metamaterial has a speed of sound relative to that of the background ($\overline{c}^*$) lower than one (upper-left region) or higher than one (bottom-right region). The symbols plot the parameters of several solid materials. It can be concluded that, for example, the propagation of sound in metamaterials based on Pb or Gel cylinders will always take place at a speed lower than that of the background, while those using Al or Poly will be larger than in the background. However, for the case of Fe, both behaviors could be possible, as the behavior depends on the filling fraction of the corresponding lattice. The horizontal (vertical) dashed line is a guide for the eye and defines the condition $c_a = 1$ ($\rho_a = 3$).

made of Pb or Gel will always result in metamaterials with $\overline{c}^* < 1$, (ii) if the cylinders in the SC are made of Al or polyethylene (Poly), their associated metamaterials will always have $\overline{c}^* > 1$ and (iii) for cylinders made of Fe, the behavior of $\overline{c}^*$ depends on f, as was already shown in figure 1.

The possibility of having metamaterials with matching of impedance with the embedded background is being looking at in many fields because of its potential application in novel devices. For example, in the field of optics a thin-film metamaterial with such a property has been recently discovered [20]. Also, it is known that anti-reflective nanostructures have been naturally developed to enhance the photon collection efficiency of the visual system in animals [21]. If such an anti-reflective effect occurs in acoustics, the transmittance at the interface between the metamaterial and background will be equal to one, although sound propagates with different speed in each medium. This property is of paramount importance in order to make useful acoustic devices like, for example, high-efficient ultrasonics transducers or powerful sonic lenses that collect all the impinging sound.

Figure 3 plots the corresponding phase diagram for $\bar{Z}^*$. The color lines represent the condition of matching of impedances, $\bar{Z}^* = 1$, for several values of f. The condition $\bar{Z}^* = 1$ is very restrictive and is very difficult to achieve for common elastic materials in bulk, only the silica Gel (a material difficult to handle) almost satisfies this condition. The acoustic impedances

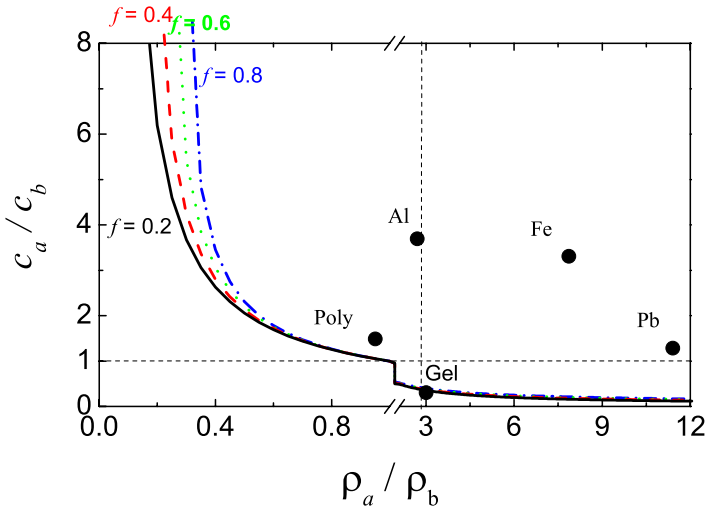

Figure 3. $c\rho$ phase diagram of acoustic metamaterials based on SC made of a square configuration of one single component elastic cylinders. For the given filling fraction, f, the corresponding color line separates the region where the metamaterial has an acoustic impedance relative to that of the background ($\bar{Z}^*$) larger than one (upper-right region) or smaller than one (bottom-left region).

Table 1. Parameters of the elastic materials studied in this work. The density, ρ_a, and the fluidlike velocity, c_a (see (8)), are normalized to those of water. However, the parameters for the silica Gel (last column) are normalized to air.

	Poly	Al	Fe	Pb	Gel
$\overline{\rho}_a$	0.95	2.70	7.86	11.40	3.00
$\overline{c}_a$	1.74	3.69	3.31	1.28	0.30

of some bulk materials are reported in table 1 and are plotted as black dots in figure 3. Note that figure 3 shows that the condition $\bar{Z}^* = 1$ could be achieved by 2D SC only if the solid cylinders are made of materials having the same property (i.e. $\overline{Z_a} \approx 1$). However, in the following section, it is demonstrated that this drawback can be overcome by using metamaterials based on a two component SC.

4. *Zc* phase diagrams for metamaterials based on 2D mixtures of two different solid cylinders embedded in a fluid

Let us consider mixtures of two different elastic cylinders of radii R_1 and R_2, respectively, that are arranged in a square configuration of side a (see inset in figure 4). The respective filling fractions are $f_1 = \pi R_1^2/(2a^2)$ and $f_2 = \pi R_2^2/(2a^2)$. If their fluidlike parameters (see section 2) are ρ_1, B_{a1} and ρ_2, B_{a2}, the resulting metamaterial has parameters determined from:

$$\zeta^* = \zeta_1 f_1 + \zeta_2 f_2, \tag{15a}$$

$$\eta^* = \eta_1 f_1 + \eta_2 f_2, \tag{15b}$$

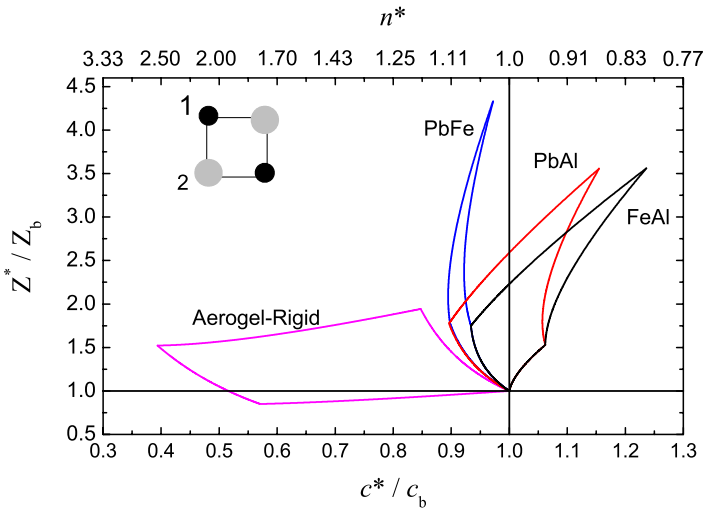

Figure 4. Zc phase diagram of acoustic metamaterials based on SC made of square arrangements of two types of solid cylinder in a background. A square lattice configuration like that displayed in the inset generates an isotropic metamaterial. The range of available relative acoustic impedances, Z^* and sound speed, c^* in the given background are defined by the area enclosed by lines with equal colors. The calculations corresponding to combinations of two metals have employed water as the background. Instead, the mixture of Gel and rigid cylinders are embedded in air. Note that the mixtures of Gel and rigid cylinders lead to metamaterials that perfectly match the air impedance. The horizontal (vertical) thin line is a guide for the eye and defines the condition $\bar{Z}^* = 1 (\bar{c}^* = n^* = 1)$.

where $\zeta_i \equiv (1 - B_b/B_{ai})$ and $\eta_i \equiv (\rho_i - \rho_b)/(\rho_i + \rho_b)$, for $i = 1, 2$. Moreover, $\zeta^* \equiv (1 - B_b/B^*)$ and $\eta^* \equiv (\rho^* - \rho_b)/(\rho^* + \rho_b)$. From these expressions:

$$\frac{1}{B^*} = \frac{1-f}{B_b} + \frac{f_1}{B_{a1}} + \frac{f_2}{B_{a2}}, \tag{16a}$$

$$\rho^* = \frac{1 + f_1\eta_1 + f_2\eta_2}{1 - f_1\eta_1 - f_2\eta_2}\rho_b, \tag{16b}$$

$$c^* = \sqrt{\frac{B^*}{\rho^*}}, \tag{16c}$$

where f is the total volume fraction occupied by both cylinders, $f = f_1 + f_2$.

The question now is, could these metamaterials accomplish the criterion of impedance matching with the surrounding background? To answer this question, let us look at figure 4 where the effective impedance $\bar{Z}^*$ is plotted against $\bar{c}^*$ for several SC made of pairs of selected materials. The calculations involving two types of metal cylinders (PbFe, PbAl and FeAl) are embedded in water while the SC made of Gel and rigid cylinders are in air. Results have been obtained under the approach $\Delta = 1$. On such a 'Zc diagram', each point on a curve obtained for a certain value f, which has associated a corresponding f_1 and f_2, represents a possible

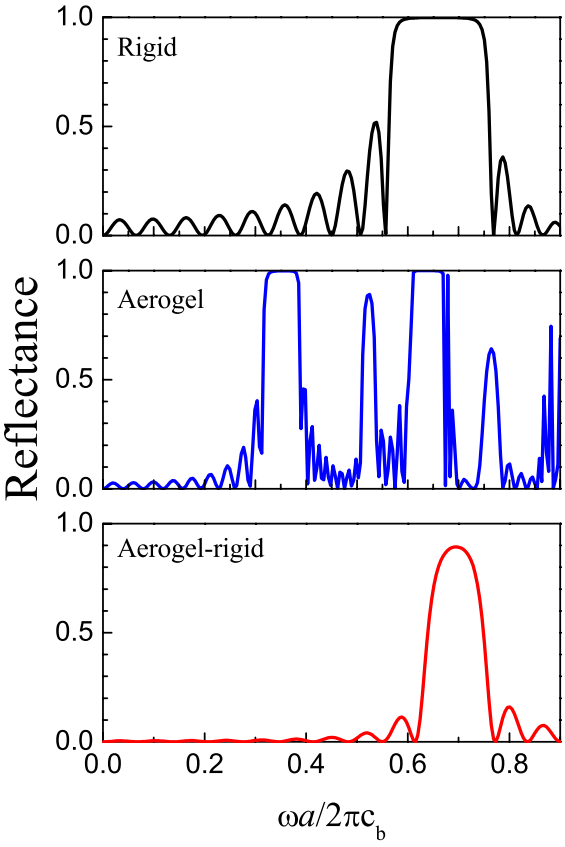

Figure 5. Reflectance of three different ten-layer slabs of cylinders distributed in a square lattice of lattice period a embedded in air and oriented along the ΓM direction. The slabs are made of rigid cylinders (top panel), Gel cylinders (middle panel) and a mixture of both (lower panel). Note how the mixture has a negligible reflectance for low frequencies.

metamaterial. The various curves obtained by changing f_1 and f_2 define an area enclosed by the parametric lines $Z^*(f_1, f_2)$ and $c^*(f_1, f_2)$. Since the larger cylinders considered have radii $R_i = a/2$, the four corners of a selected area correspond to values $(f_1 = 0,\ f_2 = \pi/8)$, $(f_1 = \pi/8,\ f_2 = \pi/8)$, $(f_1 = \pi/8,\ f_2 = 0)$ and $(f_1 = 0,\ f_2 = 0)$. The last one is always centered at the point (1, 1) in the phase diagram. Note that only the combination of Gel and rigid cylinders in air leads to a metamaterial that passes through the line $\bar{Z}^* = 1$. In other words, only this composite system is able to create a metamaterial with perfect matching of impedance with the background, which is air. Moreover, note that this remarkable property is accomplished in a broad range of filling fractions (f_1, f_2), which opens the possibility of having metamaterials transparent to airborne sound but with different refractive index.

The reflectance of a ten-layer slab made of a mixture of Gel cylinders ($f_1 = 0.015$) and rigid cylinders ($f_2 = 0.141$) put in a square lattice is shown in the lower panel of figure 5 as an example. The slab is oriented along the diagonal direction of the square lattice (i.e. along the ΓM direction); layer planes with the same type of cylinders alternate with a separation of $a/\sqrt{2}$. Note how the reflectance is almost zero or negligible in a broad range of frequencies below the first bandgap. This structure is one of many possible ones that accomplish the condition $\bar{Z}^* = 1$

in figure 4. As a comparison, the cases of slabs with the same number of layers but with one single type of cylinders, rigid or aerogel, have also been plotted. Note that for the mixture, the zero-reflectance condition is accomplished for a broad range of wavelengths; i.e., for $\lambda \geqslant 4a$ [$\omega a/(2\pi c_b) \leqslant 0.25$], which is the cutoff for the validity of the homogenization [9].

The phenomenon described above is of paramount importance because it can be used, for example, to design anti-reflective acoustic coatings, which would be similar to those recently developed for optics [20] and to build highly effective sonic lenses. Particularly, the next section shows that gradient-index sonic lenses are possible thanks to the predicted acoustic transparency (zero-reflectance) of some compound metamaterials.

5. Application: a gradient-index sonic lens

Acoustical refractive devices for airborne sound similar to those existing for optical lightwaves are not possible because solid materials are not transparent to sound waves. Also, since the sound speed of solids is larger than in air, a converging lens would have a concave rather than a lenticular shape. However, when dealing with arrays of hard scatterers embedded in air (which act as a low reflective medium at large enough wavelengths) the incident sound wave and the scattered waves are superimposed in such a way that the sound propagates at a reduced speed. Thus, Meyer and Neumann [22] were aware of these two effects and constructed a converging lens by using disks as scatterers. More recently, Cervera *et al* [1] reported a full demonstration of the focusing effect by using circular-shaped cylinders as scatterers.

The zero-reflectance property of aerogel–rigid mixed lattices described before can be used, for example, in the construction of highly effective lenticular-shaped sonic lenses by employing the procedure in [1]. However, thanks to the fact that the acoustic refractive index of the SC can be tailored without losing the zero-reflectance property, here we present the design of a gradient-index sonic lens whose functionality is based on the same effect already applied in optics [23, 24]. This novel acoustic device fully exploits the powerful properties of metamaterials based on arrays of aerogel and rigid cylinders analyzed in the previous section.

Probably the most interesting type of gradient index lens is one for which the variation in refractive index exhibits cylindrical symmetry about the lens axis, i.e. n varies only as a function of the perpendicular distance to the lens axis. For the simplest case, where the ends of the cylinder are planes perpendicular to the axis, the lens is referred to as a Wood lens, after the original inventor. As in the more general case of optics, we propose here a sonic Wood lens with a parabolic variation of the acoustic refractive index (see left panel in figure 6), thus

$$n^*(y_\ell) = n_0^* - (n_0^* - 1)y_\ell^2/(h/2)^2, \tag{17}$$

where n_0 is the refractive index on the lens axis, h is the total length on the perpendicular direction to the lens axis (i.e. y-axis), and y_ℓ defines the positions along the y-axis of the cylinders.

The designed lens is nine layers thick and consists of twenty rows of cylinders ($h/2 = 10a$) in the vertical direction with decreasing values of their radii, R_i. Maximum values correspond to the axial row ($y_\ell = 0$), where $R_1 = 0.2a$ (rigid), $R_2 = 0.3a$ (Gel) and $n_0^* = 1.31$. Minimum values are achieved in the upper and lower rows ($y_\ell = \pm 10a$), where $R_i = 0$ and $n^* = 1$. The radius of a given type of cylinders at any given row y_ℓ is determined by solving equations (15)

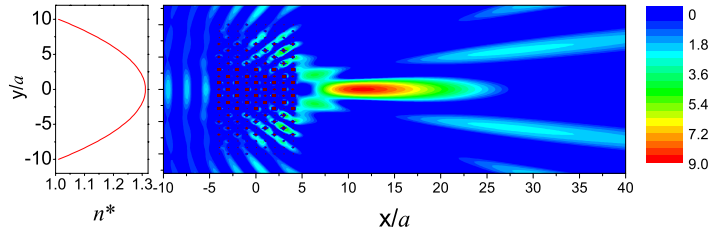

Figure 6. Right panel: sound focusing by a gradient index sonic lens made of a nine layer slab of Gel and rigid cylinders embedded in air and equally distributed in a square lattice (black dots). The pressure map in decibels ($20 \times \log|P(x, y)|$) is plotted around the lens. The sound impinges on the slab oriented along the ΓX direction. Left panel: the variation of the acoustic refractive index $n(y)$. The parabolic variation shown is achieved by decreasing the diameter of cylinders from the central row at $y_\ell = 0$ to the last upper/lower rows ($y_\ell = \pm 10a$). The working wavelength is $\lambda = 4a$.

under the condition $Z^* = 1$, which gives the following set of coupled linear equations:

$$\zeta_1 f_1 + \zeta_2 f_2 = 1 - n^*(y_\ell), \tag{18a}$$

$$\eta_1 f_1 + \eta_2 f_2 = -\frac{1 - n^*(y_\ell)}{1 + n^*(y_\ell)}, \tag{18b}$$

from which R_1 and R_2 are obtained.

The focusing effect of the proposed broadband lens is shown in the right panel of figure 6 for the case of a wavelength $\lambda = 4a$. The simulation has been performed by the multiple scattering method developed in [5, 25], where no viscosity effects are taken into account. This lens outperforms a broadband lenticular-shaped lens based on rigid cylinders [1, 5]. Thus, the ten-layer proposed lens obtains a maximum intensity of 8.8 dB at the focal point while the lenticular-shaped lens achieves only 6.6 dB by using a 19-layer thick lens.

6. Summary

We have shown that a great variety of acoustic metamaterials can be designed by using SC consisting of 2D arrangements of solid cylinders in a fluid or gas. Particularly, we reported the analytical expressions that depend on the elastic parameters of the cylinders and have proved to be very helpful in the design process. Also, for the case of two component cylinders, we have introduced Zc phase diagrams that have allowed to find metamaterials with perfect matching of impedance with air. As an application, we have reported a sonic Wood lens in which a parabolic variation of the refractive index is achieved by changing the cylinders' radii in the direction perpendicular to the lens axis. Its focusing property has been demonstrated by multiple scattering simulations and it outperforms the functionality of other lenses previously reported. In summary, our work shows that isotropic acoustic metamaterials with a broad range of possible parameters are now possible by simple means. However, the possibility of having anisotropic acoustic metamaterials for cloaking devices in acoustics [13] is still open and will be the topic of our future work. To conclude, let us also remember that a 2D acoustic system can be mapped into a electromagnetic counterpart, where P, $\vec{v}$, ρ and B correspond to H_z, $\vec{E}$, ϵ and μ, respectively. Therefore, analogous results should be expected by working with 2D photonic crystals.

Acknowledgments

We are grateful for the financial help provided by the Spanish Ministry of Science and Education (MEC) through the project no TEC2005-03545 and by Generalitat of Valencia (project no ACOMP07-204). One of the authors (DT) acknowledges a PhD grant also supported by MEC.

References

[1] Cervera F, Sanchis L, Sánchez-Perez J V, Martinez-Sala R, Rubio C, Meseguer F, López C, Caballero D and Sánchez-Dehesa J 2002 Refractive acoustic devices for airborne sound *Phys. Rev. Lett.* **88** 023902
[2] Yang S *et al* 2004 Focusing of sound in a 3D phononic crystal *Phys. Rev. Lett.* **93** 024301
[3] Fang N, Xi D, Xu J, Ambati M, Srituravanich W, Sun C and Zhang X 2006 Ultrasonic metamaterials with negative modulus *Nat. Mater.* **5** 452
[4] Krokhin A A, Arriaga J and Gumen L N 2003 Speed of sound in periodic elastic composites *Phys. Rev. Lett.* **91** 264302
[5] Gupta B and Ye Z 2003 Theoretical analysis of the focusing of acoustic waves by two dimensional sonic crystals *Phys. Rev.* E **67** 036603
[6] Li J and Chan C T 2004 Double-negative acoustic metamaterial *Phys. Rev.* E **70** 055602
[7] Hu X, Chan C T and Zi J 2005 Two-dimensional sonic crystals with Helmholtz resonators *Phys. Rev.* E **71** 055601
[8] Mei J, Liu Z, Wen W and Sheng P 2006 Effective mas density of fluid-solid composites *Phys. Rev. Lett.* **96** 024301
[9] Torrent D, Håkansson A, Cervera F and Sanchez-Dehesa J 2006 Homogenization of two-dimensional clusters of rigid rods in air *Phys. Rev. Lett.* **96** 204302
[10] Torrent D and Sánchez-Dehesa J 2006 Effective parameters of clusters of cylinders embedded in a nonviscous fluid or gas *Phys. Rev.* B **74** 223405
[11] Torrent D, Sánchez-Dehesa J and Cervera F 2007 Evidence of two-dimensional magic clusters in the scattering of sound *Phys. Rev.* B **75** 241404
[12] Håkansson A, Cervera F and Sánchez-Dehesa J 2006 Sound focusing by flat acoustic lens without negative refraction *Appl. Phys. Lett.* **86** 054102
[13] Cummer S A and Schurig D 2007 One path to acoustic cloaking *New J. Phys.* **9** 45
[14] Leonhardt U 2006 Optical conformal mapping *Science* **312** 1777
[15] Pendry J B, Schurig D and Smith D R 2006 Controlling electromagnetic fields *Science* **312** 1780
[16] Faran J J 1951 Sound scattering by solid cylinders spheres *J. Acoust. Soc. Am.* **23** 405
[17] Watterman P C 1969 *J. Acoust. Soc. Am.* **45** 1417
[18] Thorpe M F and Sen P N 1985 Elastic moduli of two-dimensional composite continua with elptical inclusions *J. Acoust. Soc. Am.* **77** 1674
[19] Wood A B 1941 *Textbook of Sound* (London: Macmillan)
[20] Xi J Q, Schubert M F, Kim J K, Schubert E F, Chen M, Lin S Y, Liu W and Smart J A 2007 Optical thin film materials with low refractive index for broadband elimination of Fresnel reflection *Nat. Photonics* **1** 176
[21] Land M F and Nilsson D E 2001 *Animal Eyes* (Oxford: Oxford University Press)
[22] Meyer E and Neumann E G 1972 *Physical Applied Acoustics* (New York: Academic)
[23] March E W 1978 *Gradient Index Optics* (New York: Academic)
[24] Evans J 1990 Simple forms for equations of rays in gradient-index lenses *Am. J. Phys.* **58** 773
[25] Sanchis L, Håkansson A, Cervera F and Sanchez-Dehesa J 2003 Acoustic interferometers based on two dimensional arrays of rigid cylinders in air *Phys. Rev.* B **67** 035422